

Optical solution for particulate distribution estimation

Original

Optical solution for particulate distribution estimation / Lombardo, Luca; Parvis, Marco; Angelini, Emma; Grassini, Sabrina. - ELETTRONICO. - 1:(2018), pp. 1-6. (Intervento presentato al convegno 2018 IEEE International Instrumentation and Measurement Technology Conference, I2MTC 2018 tenutosi a Royal Sonesta Hotel, usa nel 2018) [10.1109/I2MTC.2018.8409749].

Availability:

This version is available at: 11583/2712114 since: 2020-02-13T16:39:22Z

Publisher:

Institute of Electrical and Electronics Engineers Inc.

Published

DOI:10.1109/I2MTC.2018.8409749

Terms of use:

This article is made available under terms and conditions as specified in the corresponding bibliographic description in the repository

Publisher copyright

IEEE postprint/Author's Accepted Manuscript

©2018 IEEE. Personal use of this material is permitted. Permission from IEEE must be obtained for all other uses, in any current or future media, including reprinting/republishing this material for advertising or promotional purposes, creating new collecting works, for resale or lists, or reuse of any copyrighted component of this work in other works.

(Article begins on next page)

© 2018 IEEE. Personal use of this material is permitted. Permission from IEEE must be obtained for all other uses, in any current or future media, including reprinting/republishing this material for advertising or promotional purposes, creating new collective works, for resale or redistribution to servers or lists, or reuse of any copyrighted component of this work in other works.

Title: Optical solution for particulate distribution estimation

Authors:

Luca Lombardo

Dipartimento di Elettronica e Telecomunicazioni, Politecnico di Torino, Torino, Italy

Marco Parvis

Dipartimento di Elettronica e Telecomunicazioni, Politecnico di Torino, Torino, Italy

Emma Angelini

Dipartimento di Scienza Applicata e Tecnologia, Politecnico di Torino, Torino, Italy

Sabrina Grassini

Dipartimento di Scienza Applicata e Tecnologia, Politecnico di Torino, Torino, Italy

DOI: 10.1109/I2MTC.2018.8409749

filter surface. The system is arranged as shown in fig. 1, where the main system components are:

- A commercially available filter made in glass fiber and capable of stopping particle sizes down to $2.5 \mu\text{m}$. The filter is available either in the form of discs or as a tape and has an average pore size of $1 \mu\text{m}$. The filter appears as a white partially transparent tape which can be illuminated from behind.
- A collecting chamber which acts also as the filter holder. This chamber has been realized in ABS by using a 3D printer and its shape has been designed to allow an easy replacement of the filter and, at the same time, to make the air freely passing through the filter itself. A filter mask is employed for precisely defining the filter area where particulate matter can deposit so that the air passing per unit of area and unit of time can be precisely defined.
- A small air pump which is employed to force a constant air flux from the inlet to the sampling filter. The pump is powered in order to have a specified flux which can be changed in the range of 0.1 L/min to 0.2 L/min . This way it is possible to know the amount of air filtered by the system and such an amount can be changed according to the pollution level. The pump is connected to the collecting chamber by a small plastic tube and is located after the filter, therefore its action does not affect the particulate deposition on the filter itself.
- A back-lighting system is positioned inside the collecting chamber. This lighting system is designed to illuminate the filter from behind so that the particulate appears as black spots on a light background. The lighting system is realized by using a set of different LEDs which illuminate the filter with specified wavelengths in order to perform a sort of spectral analysis on the particulate matter deposited on the filter highlighting the presence of particulate transparent to a specific wavelengths. Two LEDs have peak emission at 880 nm , i. e. in the near infrared range and 375 nm , i.e. in the UV range, while the third one is an RGB led (625 nm , 528 nm , 470 nm) which is used to provide light in the visible range. The LEDs can be selectively turned on by the raspberry board which control the system. Thus the system works in transmission with light passing through the filter and reaching the camera. This approach has been preferred to the reflection one because it provides better image contrast and resolution.
- A cheap digital camera (Raspberry PI Camera 2) is connected to a RaspberryPI 3, a small and very cheap Computer-on-Single-Board, in order to acquire images of the filter surface and processing them. The camera features a resolution of 8 Mpixels (3280×2464 pixels) with a fixed focus lens. An additional macro lens is employed for achieving an effective resolution of about $1 \mu\text{m}/\text{pixel}$ corresponding to an effective area of about $3.2 \text{ mm} \times 2.5 \text{ mm}$. In order to reduce the cost of the system it has been selected a commercial macro-lens for



Fig. 2. The prototype of the realized measuring system. In the picture are visible: the RaspberryPI 3 used for image processing, the Raspberry PI Camera 2 module and the collection chamber with a disc filter mounted on. The plastic tube connected to the air pump is also visible at the backside of the collection chamber.

smart-phones with a magnification of $15\times$. The camera periodically takes pictures of the filter surface at the different wavelengths provided by the back-lighting system, and sends the data to the computer.

- A Raspberry PI 3 board which controls the system and provides the Linux environment which is used to perform the image processing required to identify the particulate. The advantage of using a board running the Linux operating system is the possibility of developing the image processing software on a PC running the Linux environment thus speeding up the software development.
- An image processing software, written in Python. The software, which employs the open-source openCV library [10], performs several processing on the images as described in the following section with the goal to detect the particulate matter captured on the filter, to estimate the particle equivalent size and to provide the particle distribution. The software is capable of processing the images as they are taken, therefore it is capable of increasing the accuracy in terms of counting as the time (and the amount of air through the filter) increases. In addition, a comparison among the pictures taken at different wavelengths is performed in order to provide additional information on the particulate matter composition.

A picture of one of the realized prototypes is shown in fig. 2.

III. THE IMAGE PROCESSING SOFTWARE

The image processing software is employed to perform the image analysis of the exposed filter surface as captured by the camera. The software is written in the Python programming language and uses the openCV library [10], an open source C++ library for computer vision that is available for many platforms, including Windows, Linux and Mac. The authors

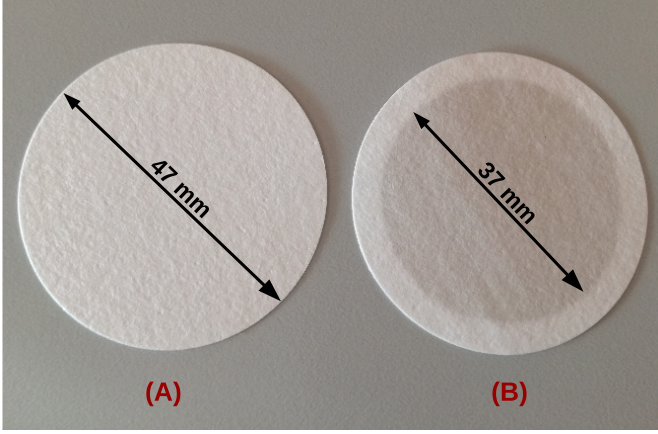


Fig. 3. The filter employed in the measurement test before (A) and after (B) an exposition of 24 h with a air flow of about 0.1 L/min. The exposed filter surface is of about 10.75 cm².

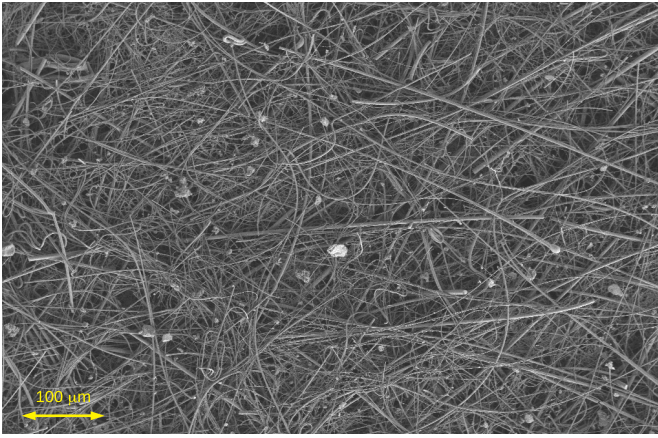


Fig. 4. Fesem image of a filter like the one of fig. 3 after the exposition to the pollutants. The filter net as well as the particles are clearly visible.

are developing different software solutions, however the current implementation relies on a solution which can be divided into two main parts: a preprocessing to clean and enhance the images and the particle recognition and clustering employing the thresholding binary matching algorithm. This algorithm generates a sequence of binary images from the original using a progressive threshold. For each binary image the algorithm detects all the features, and finally, it compares all the binary images to identify the features common to the whole sequence. A successive screening of the detected features is performed on the basis of several parameters, as the size, circularity and convexity.

The preliminary image filtering is based on three steps:

- Initially the captured image is converted into a gray-scale image. The conversion procedure depends on the actual lighting to avoid adding noise to the gray-scale image: when the IR lighting is used only the Red channel is taken into account, when the UV lighting is used only the Blue

channel is taken into account; when the lighting employs a single led of the RGB Led, the correspondent channel is taken into account. Otherwise, when multiple components are used the conversion is performed according to the equation:

$$G = \sqrt{R^2 + G^2 + B^2} \quad (1)$$

- Then a selective gaussian blurring is used on the gray-scale image for reducing the effects of the filter fibers, which can interfere with the algorithm for particle detection. In order to preserve borders of particles, a gaussian blurring is applied only to those pixels which exhibit a contrast gradient lower than a given threshold.
- Eventually a 2D kernel filtering is used for increasing the sharpness of particles in the image in a spatial selective way. This type of filtering is based on the definition of a convolution matrix K , called *kernel*, that is applied to the image. According to size and values of the matrix elements, different types of filtering can be achieved.

Several parameters have to be properly selected for achieving good identification results. In this development phase, the software allows the selection of six parameters:

- The blurring amount for preliminary image filtering (gaussian blurring) that is basically defined by the standard deviation σ in the gaussian function used in the filtering.

$$W(x, y) = \frac{1}{2\pi\sigma^2} e^{-\frac{x^2+y^2}{2\sigma^2}} \quad (2)$$

where x and y represent the spatial coordinates

- The three kernel parameters, K_0 , K_1 and K_2 , used to build the kernel matrix employed for increasing the image sharpness. The matrix used for the 2D kernel filtering is a 5×5 defined as:

$$K = \begin{bmatrix} K_0 & K_0 & K_0 & K_0 & K_0 \\ K_0 & K_1 & K_1 & K_1 & K_0 \\ K_0 & K_1 & K_2 & K_1 & K_0 \\ K_0 & K_1 & K_1 & K_1 & K_0 \\ K_0 & K_0 & K_0 & K_0 & K_0 \end{bmatrix} \quad (3)$$

The selection of the three K parameters depends on the effective back-lighting conditions and on the filter properties. In the setup employed for the characterization of the system the parameters have been selected in the following way: $K_0 = -1$, $K_1 = 2$ and $K_2 = 4$.

- The threshold range, which defines the minimum and maximum thresholds used in the binary matching algorithm for creating the sequence of binary images.
- The area which defines the range of acceptable areas for the detected particles.
- The circularity, which selects particles according to their shape or similarity in respect to a circle. The circularity parameter C is defined as:

$$C = \frac{4\pi A}{P^2} \quad (4)$$

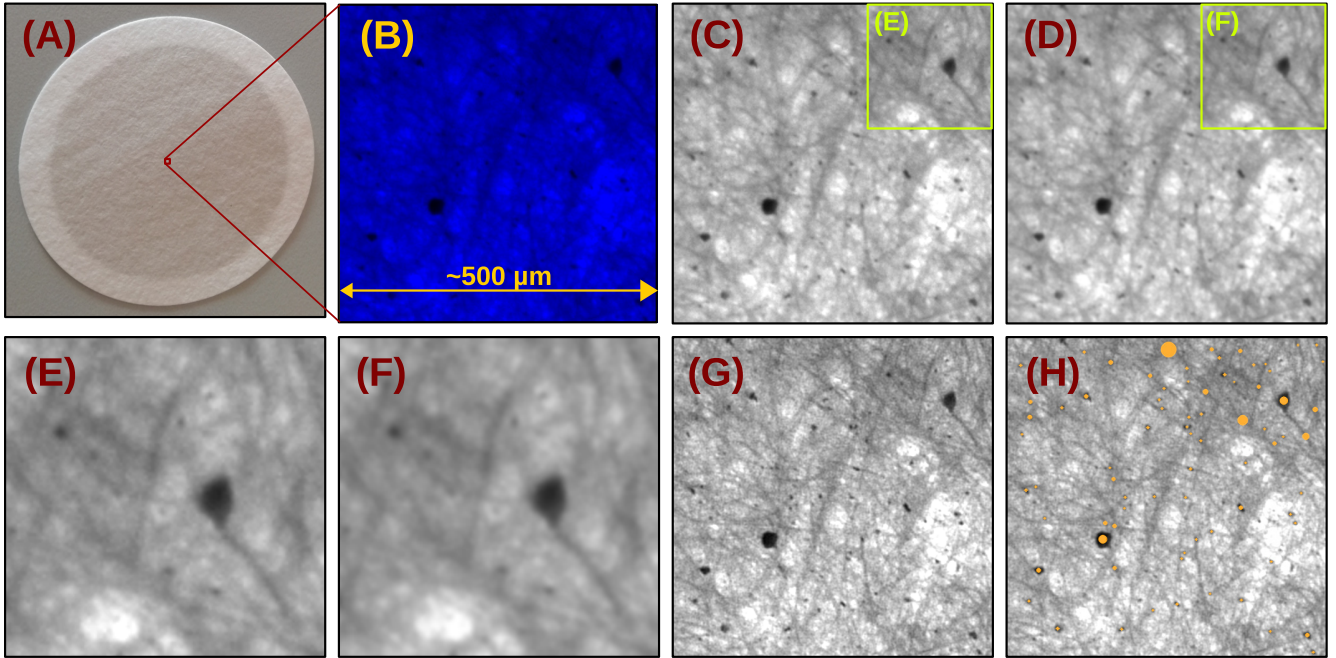


Fig. 5. (A) the filter employed in the measurement test after a 24 h exposition with a air flow of about 0.1 L/min. (B) the blue channel of image as captured by the camera with an UV back-lighting; (C) the gray-scale image, (D) the image after application of the selective gaussian blurring, (E) a detail of the gray-scale image, (F) the same detail after the blurring, (G) the image after the 2D kernel filtering and (H) the map of detected particles.

where A and P are, respectively, particle area and perimeter.

- The convexity, which defines the minimum and maximum allowable convexity for selecting a particle.

All these parameters can be manually selected by the user during the system calibration. A user-friendly graphical user interface (GUI) is available for adjusting such the parameters interactively using sliders.

IV. RESULT AND DISCUSSION

The measurement system described in this paper is actually under development in order to improve performance of both the optical detection system and the processing software. Anyhow, several tests have already been carried out in real environmental conditions. Measurements have been performed in different locations in north and south of Italy and some of the results are reported here.

In these preliminary measurement a commercial GF10 circular borosilicate glass fiber filter with a diameter of about 47 mm and thickness of about 350 μm has been employed. The filter mask, which fixes the filter itself on the collecting chamber has a diameter of about 37 mm. Fig. 3 shows the filter aspect before (A) and after (B) an exposition of 24 h with an air flow of about 0.1 L/min carried out in a medium polluted city in north of Italy. The change in color of the filter after the exposition is clearly visible. Fig. 4 instead shows an image of a filter like the one of fig. 3 taken with a field emission scanning electron microscope (FESEM) which has an extremely high resolution. The image clearly shows the

particles, but also highlight the presence of the borosilicate wire network, which realize the filter and which makes it difficult to realize a software capable of isolating the single particles.

Fig. 5 shows the processing steps carried out on the filter exposed during one of the initial tests and shown in fig. 3.

Image A shows the filter after the exposition to the pollutant, image B shows the blue channel of a small portion of the image section captured by the camera and taken with an UV back-lighting. The shown image portion is of 500×500 pixels corresponding to about $500 \mu\text{m} \times 500 \mu\text{m}$.

Image C shows the gray-scale version of image B obtained by processing only the blue channel as described before and image D shows the same image after the gaussian blur which is employed to reduce the filter net disturb. The images look similar even though the filter net is clearly reduced in the D image therefore helping the subsequent identification. This reduction is clearly visible in the two details E and F taken respectively from the gray-scale and blurred images.

Image G shows the sharpening effect provided by the processing with the 5×5 kernel. Eventually image H shows the particle detection map generated by the software. Each detected particle is marked with a circle whose diameter represents the estimated average size of the particle itself.

The possibility of using lights of different wavelengths is conceived to let users to roughly distinguish between different types of particles. In principle, the transparency of the collected particles changes according to their composition and wavelength used. Thus, taking several images of the same filter

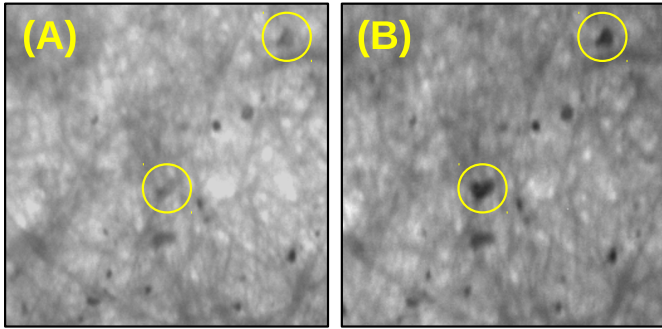


Fig. 6. Comparison of two images of the same filter area taken by the camera with infrared (A) and UV (B) backlighting. The two marked particles exhibit a different transmissivity at the two wavelengths

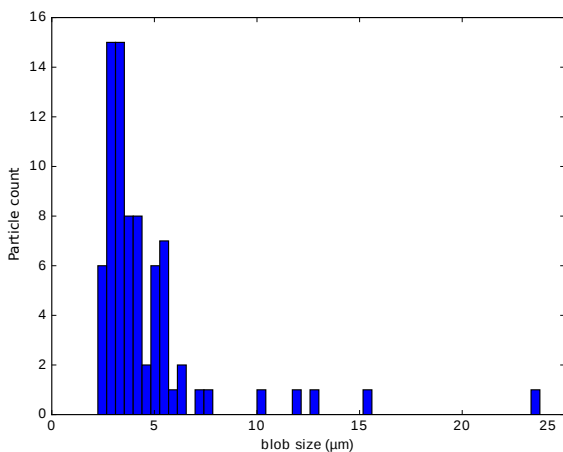


Fig. 7. Histogram reporting the particle size distribution as detected by the software. The peak of particle distribution is at a size of $3 \mu\text{m}$.

area at the different wavelength provided by the back-lighting system can be very useful to discriminate between the different compositions.

As an example, fig. 6 shows the same filter area captured with infrared light (A) and with UV light (B). For some particles, specifically the ones marked by the yellow circles, a clear difference is visible, while for the other particles no difference is visible.

Using the identified particles and their equivalent size, it is easy to compute the particle distribution. As an example, fig. 7 shows the histogram of particle size distribution, as generated by the detection software on the images of fig. 5. In this case the histogram shows that the peak of particle distribution is at about $3 \mu\text{m}$ highlighting how a health risk still exists even though the $10 \mu\text{m}$ (i.e. the PM10) particle presence is rather low.

V. CONCLUSIONS

The preliminary results obtained by using the proposed system are very promising for the development of a low-cost

monitoring system for atmospheric particulate matter, which is able to estimate not only the total amount of particulate, but also its size distribution.

The measurement system is actually under development and its characterization is being performed by using the images obtained by a FESEM, which allows one to obtain resolutions of few nanometers, equipped with an energy dispersive spectrometer (EDS).

The FESEM/EDS analysis allows one assessing morphology and chemical composition of the particulate matter, but unfortunately the processing of the FESEM images is difficult due to the borosilicate wire presence, which prevents a direct use of an image analysis software. The authors are currently working on a mixed manual/automatic solution to obtain a particle distribution from the FESEM images.

The authors are also working on the improvement of both the optical system and the detection software trying to implement image subtraction procedures between the filter image before and after exposure for reducing the influence of the filter fibers on the particle detection. This effect has been observed to be the main interference problem for the correct particle detection and requires a careful selection of the blurring parameters. The subtraction based procedure should avoid most of these problems, but requires a highly stable setup.

Also, the selection of the parameters is crucial for the improving performance, but these change with the filter and the back-lighting. For this reason an adaptive estimation of these parameters is being developed. Finally, a filter motion system is being added to the proposed system in order to automatically change the filter when required.

REFERENCES

- [1] C. Chiang "Design of a High-Sensitivity Ambient Particulate Matter 2.5 Particle Detector for Personal Exposure Monitoring Devices", IEEE Sensors Journal, Vol. PP, no.99, 2017, pp. 1-1
- [2] M. B. Marinov, S. Hensel, B. Ganev, G. Nikolov "Performance evaluation of low-cost particulate matter sensors", 2017 XXVI International Scientific Conference Electronics (ET), 2017, pp- 1-4
- [3] R. M. Carter; Y. Yan "An instrumentation system using combined sensing strategies for online mass flow rate measurement and particle sizing", IEEE Transactions on Instrumentation and Measurement, Vol. 54, no. 4, 2005, pp. 1433-1437
- [4] R. M. Carter, Y. Yan, P. Lee "On-line Nonintrusive Measurement of Particle Size Distribution Through Digital Imaging", IEEE Transactions on Instrumentation and Measurement, Vol. 55, no. 6, 2006, pp. 2034-2038
- [5] X. Yu, Y. Zhi, B. Li, Q. Gong, Y. Xiao "Size spectrometry of environmental particulate matter using a nanofiber array", 2017 Conference on Lasers and Electro-Optics (CLEO), 2017, pp. 1-2
- [6] E. Sisinni, A. Depari, A. Flammini, "Design and implementation of a wireless sensor network for temperature sensing in hostile environments", Sensors and Actuators A: Physical, January, 2016, Vol. 237, pp. 47-55, ISSN 0924-4247, DOI 10.1016/j.sna.2015.11.012.
- [7] L. Ascorti, S. Savazzi, G. Soatti, M. Nicoli, E. Sisinni, S. Galimberti, "A Wireless Cloud Network Platform for Industrial Process Automation: Critical Data Publishing and Distributed Sensing", IEEE Trans. Instrumentation and Measurement, February, 2017, Vol. 66, N. 4, pp. 592-603
- [8] L. Lombardo, S. Corbellini, M. Parvis, A. Elsayed, E. Angelini, S. Grassini, "Wireless Sensor Network for Distributed Environmental Monitoring", IEEE Transactions on Instrumentation and Measurement Early access article, December 2017

- [9] S. Corbellini, E. Di Francia, S. Grassini, L. Iannucci, L. Lombardo, M. Parvis "Cloud based sensor network for environmental monitoring", Measurement: Journal of the International Measurement Confederation, Early access article, 2017
- [10] OpenCV library available at <https://opencv.org>, last checked on Dec. 5, 2017